University of Texas at Arlington

MavMatrix

8-10-2022

Supplementary Information for "Understanding Mid-to Large Underground Leaks from Buried Pipelines as Affected by Soil and Atmospheric Conditions – Field Scale Experimental Study"

Navodi J.R.R. Jayarathne
University of Texas at Arlington

Kathleen M. Smits
University of Texas at Arlington

Stuart N. Riddick
Colorado State University - Fort Collins

Daniel J. Zimmerle
Colorado State University - Fort Collins

Younki Cho
University of Texas at Arlington

Recommended Citation

Authors

Navodi J.R.R. Jayarathne, Kathleen M. Smits, Stuart N. Riddick, Daniel J. Zimmerle, Younki Cho, Michelle Schwartz, Fancy Cheptonui, Kevan Cameron, and Peter Ronney

Supplementary Information for Understanding Mid-to-Large Underground Leaks from Buried Pipelines as Affected by Soil and Atmospheric Conditions – Field Scale Experimental Study

J. R. R. Navodi Jayarathne[1], Kathleen M. Smits[1], Stuart N. Riddick[2,3], Daniel J. Zimmerle[2,4] Younki Cho[1], Michelle Schwartz[1], Fancy Cheptonui[2,4], Kevan Cameron[2], Peter Ronney[2,3]

[1]Department of Civil Engineering, University of Texas Arlington, Arlington, Texas
[2]Energy Institute, Colorado State University, Fort Collins, Colorado
[3]Department of Mechanical Engineering, Colorado State University, Fort Collins, Colorado
[4]Department of Systems Engineering, Colorado State University, Fort Collins, Colorado

Supplementary Material Section 1: METEC Rural and Urban testbeds

S1.1 METEC Rural testbed

The rural testbed is the field scale test facility designed to understand the transient behavior of subsurface, surface and atmospheric development of NG plumes due to mid and large-scale underground NG leaks.
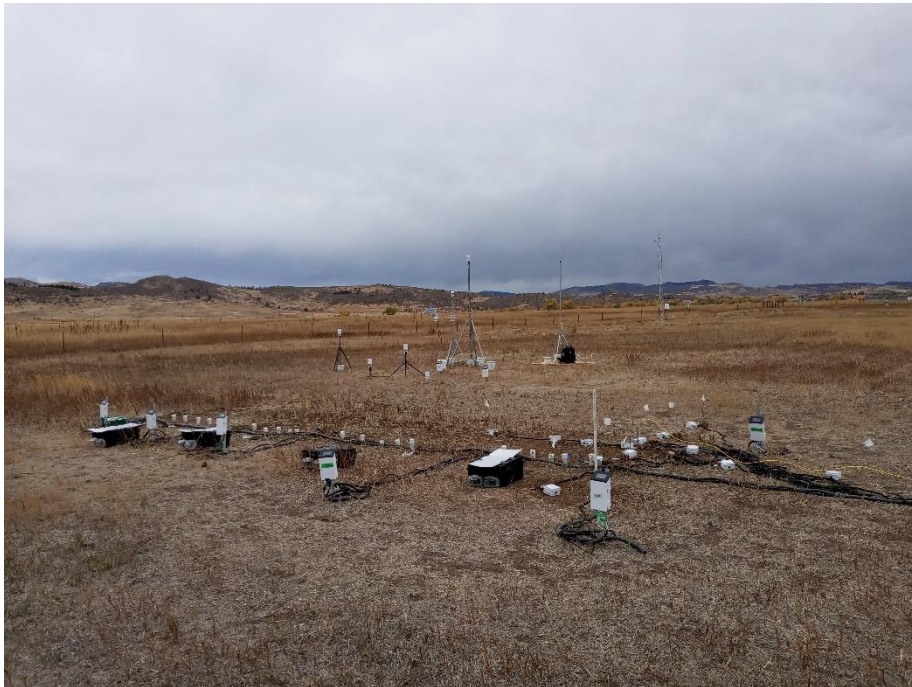

Figure 1: View of METEC rural testbed during an experiment. All subsurface, surface, and atmospheric CH$_4$ sensors are in place along with environmental sensors.

The test bed is capable of releasing NG of differing compositions (combinations of methane, ethane, propane, and butane) at rates up to 300 slpm from underground release pints installed at two different depths. The release points were installed as two pairs (North pair and South pair), with each pair having 1.8 m BGS and 0.9 m BGS release points. This 30 m long testbed has the capability of measuring the subsurface migration of natural gases up to 30 m distance from the release point. Figure (2) below shows the subsurface vertical section of the testbed. Subsurface CH_4 measurements were conducted using 30 SGX INIR-ME100% sensors (hereafter referred to as INIR sensor) placed at three different depths of 1.8, 0.9, and 0.3 m below ground surface (BGS) at six different locations. At each location, there were 2 sensors at 1.8 m, and 0.9 m depths while 0.3 m had a single sensor.
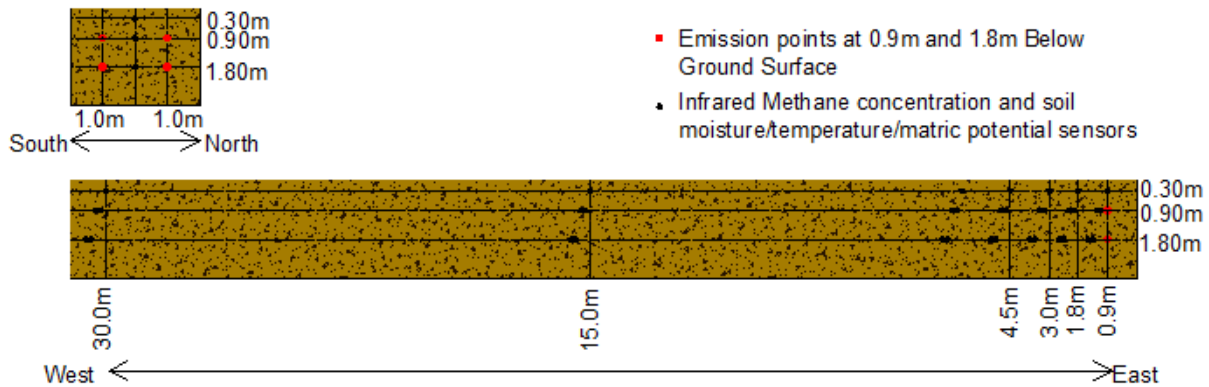
Figure 2: Schematic of the Rural testbed profile with locations for belowground Emission points and sensor locations for Infrared Methane (INIR), Soil moisture/temperature/matric potential sensors. Specific distance from emission point and depths from surface are also shown.

The testbed is further equipped with subsurface and atmospheric environmental to measure soil moisture, temperature and matric potential using TEROS10, TEROS11, and TEROS21 (METER Group, Inc.; USA) respectively and atmospheric measurements as wind speed, air temperature, precipitation, barometric pressure including 10+ more variables using ATMOS41. Subsurface sensors were permanently installed at each depth (Figure 2) while atmospheric environmental sensors were placed at 0.05 m and 0.3 m above ground surface in a semi-permanent (height specific for this experimental series) basis. Detailed descriptions on sensor selection, design, calibration, field performance, field deployment, data extraction and processing can be found from INIR sensors (section 2.2) and environmental sensors (section 2.6).

S1.2 METEC Urban testbed

The urban testbed is the field scale test facility designed to understand the transient behavior of subsurface, surface and atmospheric development of NG plumes that are arising due to mid-to-large scale (leak rates > 2.2 slpm) underground NG leaks occurring around urban and suburban environments. This is a 100 m long and 15 m wide test facility with three structures, a road and other urban characteristics constructed with a required sensor facility as shown in Figure 3 below.

Figure 3: View of METEC Urban testbed showing Structure1 (Concrete slab foundation), Structure2 (Basement), Structure3(Crawlspace), the road running through the testbed and the Asphalt pavement infront of Structure2.

Each structure comprises three pairs of release points all at 0.9 m below ground surface (Figure 4) Each pair of emission points simulate subsurface gas leaks adjacent to each of three structures, the structure's foundation differ and represent those typical to the USA – basement, crawlspace and slab foundation (PHMSA, 2020). More specifically, structure 1 (East structure) has a concrete slab, Structure 2 (Middle structure) has a basement and Structure 3 (West structure) has a crawlspace as their substructures. The concrete slab is a 0.1 m thick 1.8 m x 1.8 m set on the ground, the basement is 0.9 m deep with a 0.1 m thick 1.8 m x 1.8 m concrete floor and cinder block walls (Figure 3) and the crawlspace consists of a single layer of cinder blocks. The three structures (1-3) are constructed as wooden sheds with the same footprints as the foundations. All three

structures are aligned 3.5 m south from the road running East-West direction of the testbed. The three structures are located far enough as not to interfere with releases from other two (Figure 3).

Adjacent to each structure are two NG release points located 0.9 m BGS, and 5.5 m away from the edge of the foundation (Figure 4). The depths of the emission points were selected based on soil cover requirements for NG distribution mains which ranges from 24 to 48 inches, depending on the type, class and location of the pipeline (Electronic Code of Federal Regulations §192.327 Cover, 2021)

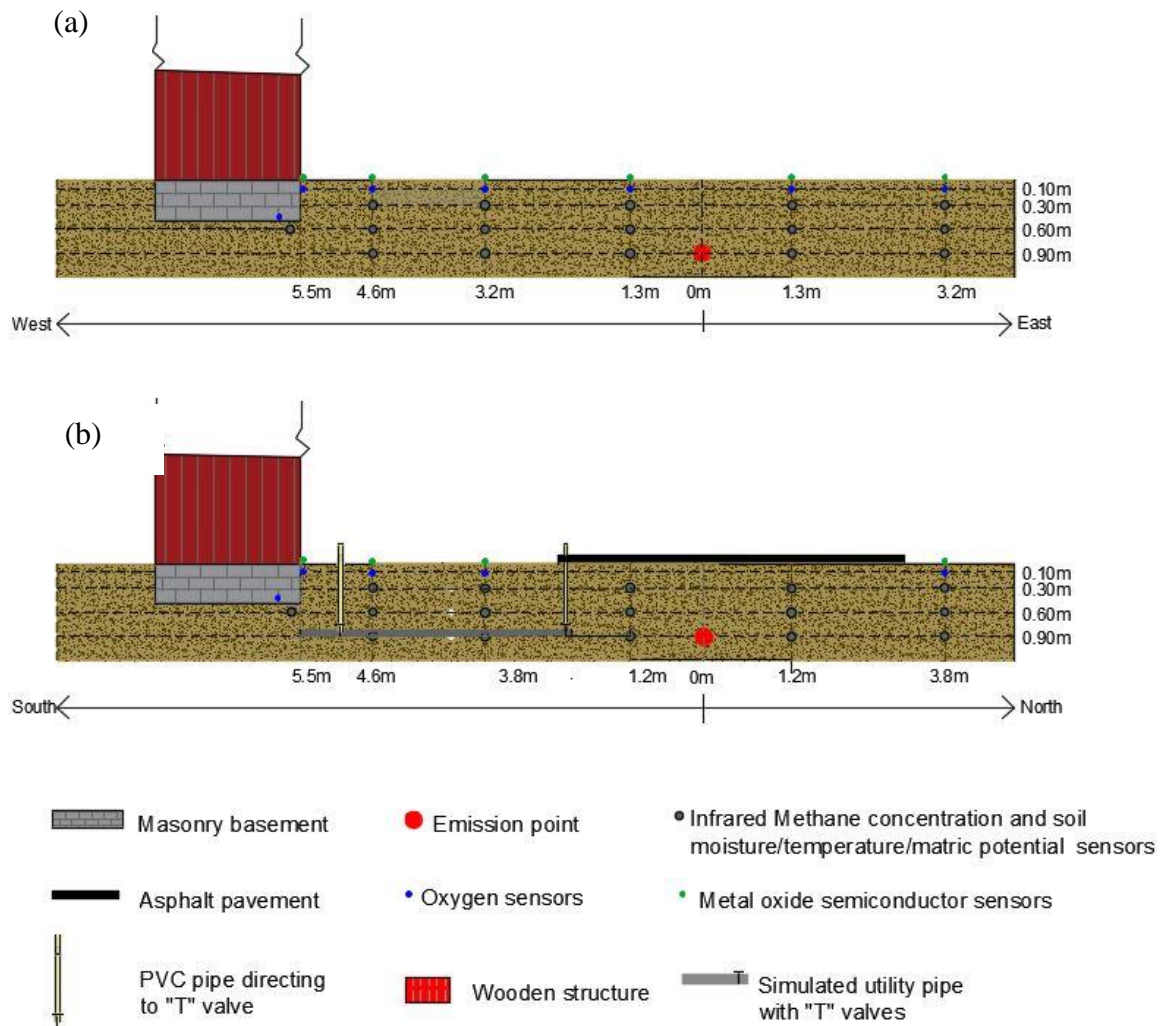Figure 4: Schematic of the test bed profile for the Structure 2 with a basement. The location of gas release points, asphalt pavement and the utility pipeline and the location for each type of sensors are also shown. (a) East – West profile in which a NG release point is located 5.5 m from the building foundation with a grassy surface and (b) North-South profile in which the release point is located underneath a paved road.

Around each structure there exist two buried utility conduits at 0.9m depth, running from the road towards the structure as shown in the figure (4), are used to simulate urban and suburban subsurface. One 0.05 m diameter pipe buried at 0.9 m has a valve at both ends and can be selectively closed to simulate an empty communication or sewer line (urban environment) or a sealed pipe (suburban environment) and is equipped with a valve at either end that can open or close (suburban environment). The second pipe, 0.1 m diameter and sealed at both ends, was laid alongside the first. It is important to note that the belowground installation of the utility conduits was performed similarly to the commonly practiced pipeline installation procedures, i.e., a trench of 0.3m wide and 0.9m was created for laying the pipe and then backfilled with native soil followed by compaction.

A 2.3 m wide and 15 m asphalt paved road was laid 5 m from the "basement" structure (Figure 4). In addition to asphalt, other surface coverings include semi permeable artificial grass (AstroTurf) and movable impermeable AM2 matting, consisting of steel rectangles coated with an epoxy nonskid material that can be assembled in a brickwork pattern to form different surface configurations (e.g., sidewalk) that can be configured in accordance with each experiment.

We used numerical models and previous experimental results to determine the optimal sensor locations to capture of the movement of underground NG plume. Accordingly, sensor locations were selected up to 9.3 m Northward and 8.7 m Eastward from the edge of the foundation along 5 vertical cross sections as shown in Figure (4). Each vertical section consists of sensors at five different depths of 0.9 m, 0.6 m, 0.3 m, 0.1 m and 0m (surface) BGS. The deeper three depths ensure the equi-spaced cover age while 0.1 m and surface level sensors allow for the near surface understanding of the gas flow and transport. Two additional sensors were installed underneath the foundation. All environmental sensors are installed permanently while the methane sensor installation is semi-permanent, allowing for periodic removal for calibration. 0.9 m, 0.36 m, and 0.3 m BGS CH_4 concentrations were measured using INIR sensors while 0.1m CH_4 measurements were based on an oxygen replacement method (described below) and surface measurements were conducted using Natural Gas (NG) detectors units designed for CH_4 measurements. Environmental parameters of soil moisture, temperature and matric potential were measured using TEROS10, TEROS11, and TEROS21 respectively and ATMOS41 sensors (installed at 0.05 m, 0.5 m, and 1 m above ground surface) were used for atmospheric parameter measurements. Readers are encouraged to refer INIR sensors (section 2.2), oxygen replacement method (section 2.4), NG detectors (section 2.3), and environmental sensors (section 2.6) for detailed descriptions on sensor selection, design, calibration, field performance, field deployment, data extraction and processing.

S1.3 Belowground Release points and Controlled releases

The release points were fabricated using a 0.635 cm vent screen (model SS-MD-4, Swagelok, USA) surrounded by a 10 cm wire cube filled with gravel to prevent clogging. It is to note that the above procedure was specifically followed during construction of all METEC belowground release points. The vent screen was then connected to 0.635 cm PTFE tubing connecting it to the NG flow control system. Compressed NG with methane compositions ranging from 85%vol – 95%vol methane are provided from two 145 L cylinders. Importantly, the composition of the NG can further be adjusted to have different compositions of methane, ethane, propane, or butane when required. NG to the tanks were supplied from the city gas supply as a compressed natural gas (CNG). This is a process that involve a gas compressor and a transport truck. The gas compressor unit at PowerHouse (CSU, Fot Collins, CO) pumps the gas from the city gas supply at 20 psi to 3600 psi and transfers to the METEC CNG truck. The truck then transfers CNG to METEC 145 L cylinders, mixing it with the remaining gas. The composition of the new mixture was then determined using a gas sample analyzed by chromatograph.

The flow from the cylinders is controlled using pressure regulation and solenoid valves in series with precision orifices, allowing for the controlled emissions. The mass flow rate was controlled using pressure regulation and several solenoid valves in series with precision orifices, and was monitored using either a 0-15 slpm or 0-75 slpm mass flow meter (Omega FMA1700 series). The control systems are placed inside Gas Houses constructed near each testbed and are weather insulated in order for uninterrupted experiments during extreme weather conditions. Details of the control system design and operation can be found in Bell et al. (2020) and Zimmerle et al., (2020).

Supplementary Material Section 2: Sensor technology

S2.1 Methane Sensor selection

METEC rural and urban testbeds are the METEC's first long term belowground sensor deployment for all season measurements. The selection of a sensor for belowground CH_4 measurements was based on a comparison of technical and cost details among the sensors available in the market. Shown below are the property comparison of CH_4 sensors. To be able measure the speed and distance of gas in the subsurface, CH_4 sensors were installed below ground at depths of 0.3, 0.6, 0.9 and 1.8 m at selected distances from the leak point (Figure 2 and 4), preference was given to smaller sensors. Required detection range was from 500 ppm up to 10^6 ppm (100%) CH_4. Due to the climate in Colorado, the sub-surface CH_4 sensors needed to operate at temperatures between -20 and 50 °C and in a relative humidity between 30 and 100%. Additionally, ~50 sensors were deployed, therefore, the sensors needed to fit in the budget. Seven CH_4 concentration technologies were investigated (Table 1) and the SGX Sensortech INIR-ME100% was selected for use.

Table 1: CH_4 sensor property comparison

Instrument	DOD New Cosmos BGS	Sensit CGI	Sensit PMD	Gas Rover	Figaro Oxygen	Figaro TGS2611	Nenvitech IRNEX-P	Sensortech INIR-ME
Technology	Thermal Conductivity	Semi conductor sensor	IR	CC/TC sensor	Galvanic cell	MOS	IR	IR
Above/ belowground	Below	Both	Both	Both	Above	Above	Above	Above
Range		0 to 100%	1 to 100%	2 to 100%	-	0 to 1%	0 - 100%	1 - 100%
Accuracy		±5%	±10%	±10%	±1%	±25%	±5%	±5%
Data logging	CR1000	Yes	Yes	Yes	External	External	External	External
Size of sensor (cm^2)		200	250	5	11.28	0.8	3.14	3.14
Will it work below ground	Yes	Maybe	Maybe	Yes	-	No	No	no
T operating range (°C)	-10 to 40	-20 to 40	-20 to 50	-20 to 40	5 - 40	-40 to 70	-40 to 60	-40 to 75
RH operating range (%)	0 to 85				0 to 95	10 to 90	35 to 95	0 to 95	10 to 90
Response time		< 60 s	< 3 s	<0.5 s	15 s	30 s	≤ 30 s	≤ 30 s
Price ($)	$2,700	$2,200	$11,000	$4,000	$80.00	$16	$350	$250

S2.2 SGX INIR-ME100% sensor

Description

The SGX Europe (Katowice, Poland) Integrated Infrared (INIR) CH_4 sensor, INIR-ME100%, is designed to measure CH_4 concentrations in air from 100 ppm to 100% CH_4 by volume (bv). in temperatures from -40 to 75°C and relative humidity from 0 to 99% that can output data as either a digital or analog signal. The sensor is contained in a stainless-steel housing (diameter 20 mm, height 17 mm) that has a 5-pin polygon socket (5 mm pins) to supply power and transmit data to and from the INIR sensor. The pin configuration is as listed below:

1. TXD: Data transmitted from the INIR
2. VCC: 3.2 Volts – 5.25 Volts DC input to INIR
3. GND: 0 Volts reference for INIR
4. RXD: Data received by the INIR
5. OUT: Analogue output

Calibration procedure

During calibration, the SGX "Smart IR Evaluation Kit" software and "Smart IR" configuration kit were used. The sensor was plugged into the evaluation board, which was connected to a computer. The software GUI was used to communicate with the INIR sensor and display the sensor's output signal during calibration. Following manufacturer instructions, the INIR sensor was inserted into a cap with fixtures to allow calibration gas to be passed over the sensor. Calibration comprised of a zero calibration, a high span calibration and target calibration:

1. Zero calibration: 100% Nitrogen gas was connected to the INIR sensor and left for 45 minutes. When the readings stabilized the sensor output was recorded by the INIR as zero.
2. High span calibration: After the zero calibration, 20% CH_4 gas was connected to the calibration cap inlet and left to run for 5 minutes until readings stabilize. After the readings had stabilized the output value was recorded by the INIR sensor as 20%. 100% Nitrogen was reconnected for 5 minutes.
3. Target calculation: 2% CH_4 gas was connected to the sensor and left to flow for 5 minutes. After the readings had stabilized the output value was recorded by the INIR sensor as 2%. 100% Nitrogen was reconnected for 5 minutes.

Sensor stability in air and soil

Sensor testing was done to characterize the accuracy of the INIR sensor in air and soil using calibration gases with CH_4 concentration of 400 ppm, 5,000 ppm, 5%, 50% and 100% by volume. To test the sensor response in air, the CH_4 mixes were flowed over the INIR sensor using the calibration cap. Nitrogen was passed over the INIR sensor between each measurement to flush

the existing CH_4. The INIR sensors showed good linearity between 5,000 ppm and 100% but underestimated lower concentrations (Figure 5).

To test the sensor response in dry soil, the soil was first dried for 24 hours in an oven. The dry soil was then packed into a 2" PVC tube which had fixtures to allow gas to flow through the soil and was sealed at the top. The INIR sensor was placed in a holder which sealed the open end of the tube. Similar to the sensor in air, the INIR sensor's response is linear between 5% and 100%. The INIR sensor underestimated lower concentrations in soil, 500 to 5,000 ppm (Figure 5)

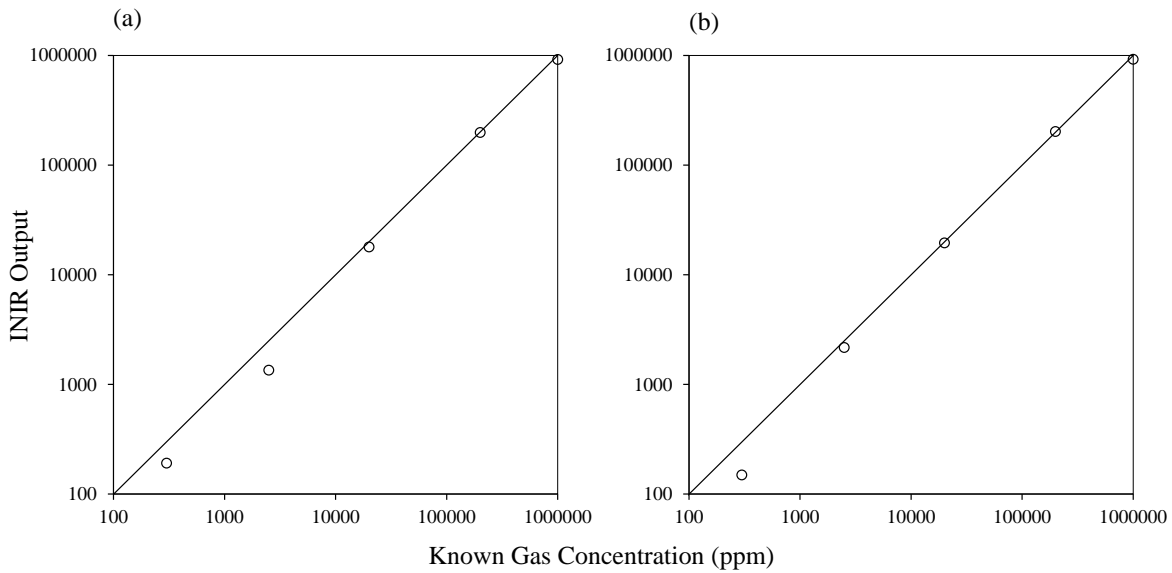*Figure 5: Six-point calibration of the SGX INIR-ME 100% sensor in (a)air and (b) dry soil*

<u>Sensor response rate</u>

The response time of the INIR was measured by passed 500 ppm CH_4 gas through the calibration cap and measuring the time it takes for the sensor output to reach 90% of the maximum value from background (T90). The T90 response time for the INIR sensor was 10 seconds (Figure 6).
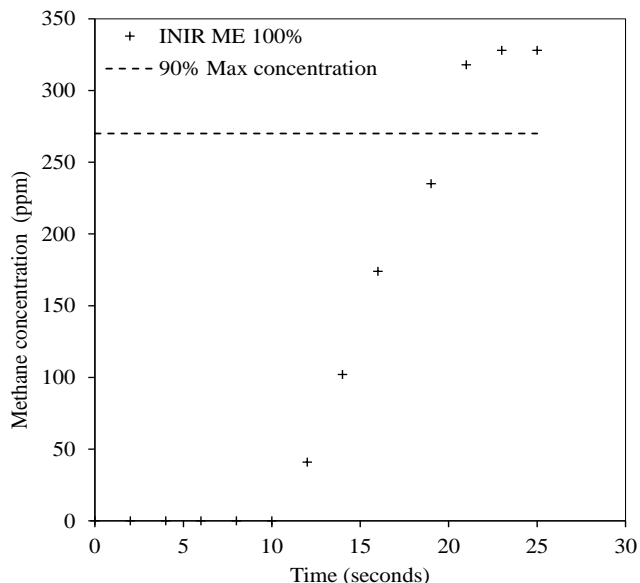
*Figure 6: Response rate of the INIR ME100% sensor
between 0 and 300 ppm*

Field performance

Field performance evaluation of INIR sensor was conducted at METEC after improving an existing testbed to deploy INIR sensors. The improved testbed for field performance testing had vapor implants installed at pre-determined depths and PVC sleeves collocated with vapor plants. A 10.8 slpm CH_4 leak was simulated using a release point installed at 0.9 m depth and continued for 5.6 hrs. INIR sensors (Table 1) were allowed to measure the subsurface methane concentration variation continuously throughout the entire experimental period. 9.2 ml of gas samples were collected as per ASTM D7648-12 from vapor implants at selected time intervals (Before release initiate, 30 min, 1 hr, 2.25 hr, and 4 hrs after starting the release) to represent the transition and steady states of methane plume buildup. The results from INIR sensors were compared with independent gas analysis results obtained from vapor implant samples analyzed using gas chromatography (GC). The results of the field testing are shown in Figure (7) below. As per the results methane concentration values followed similar trends, demonstrating the validity of the INIR method for use with our field experiments for continuous measurement of subsurface methane concentrations.
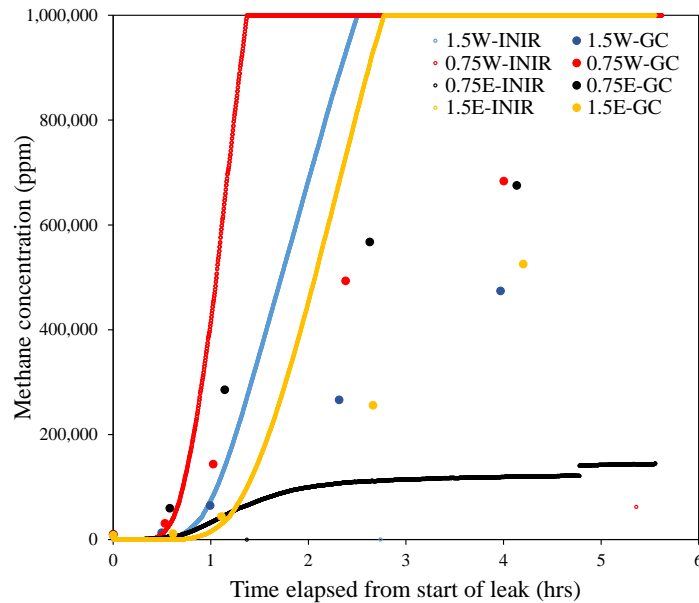
Figure 7: Methane concentration as measured by INIR sensors (small scatter points) and Gas Chromatography (large scatter points) for 1.5m West (1.5W), 0.75m West (0. 75W), 0.75m East (0.75E), and 1.5m East (1.5E) measuring locations

Field deployment and installation

As the INIR sensors needed to be removed between experiments, they were mounted to a stainless-steel holder custom designed for the sensor dimensions. The stainless-steel holder consists of a 4.6 cm diameter solid cylinder with a hollow bottom to hold the cylindrical 2 cm diameter by 1.3 cm long INIR sensor (Figure 8). The sensors were connected to data acquisition (DAQ) units using a bespoke 5-pin connector. The stainless-steel holder was sealed against the PVC sleeve using an O-ring and the wire connecting the sensor was protected using ¼ inch stainless-steel tubing from the stainless-steel holder to the surface.

Figure 8: The Stainless-steel holder and 1/4 tubing assembly for INIR-data wire protection

Data acquisition

All the raw data from the INIR sensors are transferred to a DAQ unit (Figure 9). Each DAQ unit collected data from five INIR sensors. The wire from the INIR was connected to the DAQ unit via a 5 pin IP68 aviation connector and UART data were then passed to a Panasonic Toughbook personal computer (Panasonic USA) via a USB to TTL adapter. Data were read using a python code, stored on the DAQ and also uploaded to a shared cloud platform. Data were available remotely 20 s after being read by the INIR sensor. The DAQ unit was housed in an IP68 plastic case enabling them to stand out at the field during extreme weather conditions.

Figure 9: A Data Acquisition (DAQ) Unit placed at the testbed during an experiment. The Toughbook computer, the data flow connections of 5 pin IP68 aviation connectors can also be seen.

Standard operation procedure

After the sensors are installed and connected to the DAQ units, computers are powered up by connecting to the general power supply. Required power outlets are installed at specific locations within the testbeds. It is advised to power up the computers and switch them ON after completing the sensor-DAQ connections. The specific python code for sensor-data acquisition is installed with a shortcut to appear on the computer desktop.

Data analysis

As the data are directly recorded in ppm terms in to *.txt* files, the user can transform to any file format of preference. The only requirement will be to select the correct sensor and the specific period of testing.

S2.3 Natural Gas (NG) detectors for Surface CH$_4$ measurement

Natural Gas detector consists of a metal oxide semiconductor (TGS2611-E00, Figaro) that detects methane from 500-10,000 ppmv range and uses tin oxide (SnO$_2$) as the gas sensing material. This metal oxide sensor (MOS) was specifically selected due its accuracy and cost. Because the MOS sensor is sensitive to relative humidity and temperature, the NG detector is equipped with relative humidity and temperature sensor (SHT35-DIS-F2.5Ks, Sensirion AG) to account the effects on the MOS sensor. In addition, a piezoresistive absolute pressure sensor in the NG detector measures atmospheric pressure (LPS25HB, STMicroelectronics).

Performance and Calibration

A calibration algorithm for the MOS sensor was previously developed by calibrating at 8 gas concentrations (0, 10, 50, 100, 500, 1000, 5000, and 10,000 ppmv) under 3 temperatures within the range of (28.5 – 40.6 °C) and relative humidity from 5 % to 60 %. Temperature and relative humidity ranges were selected to represent the field conditions as observed by METEC MET station. The performance of calibration algorithm for the MOS sensor was evaluated with a cavity ring-down spectrometry analyzer (G4302 GasScouter, Picarro, Inc.), and it was proven to be complying with an average R^2 of 0.96 using 100s time interval averages when the two measurements were compared. A successful field trial of the NG detectors at METEC in May 2020 demonstrated applicability under dynamic environmental conditions that are likely to experience during NG pipeline leak surveillance. In the field trial, the leak rates selected for the testing were 0.042 and 0.127 kg h^{-1}.

All the sensors were calibrated at the lab before field deployment using the same calibration algorithm, and periodic calibrations were conducted every three months or after a long isolation period.

Filed Deployment and Installation

Filed deployment of NG detectors followed the same location selection criteria as oxygen sensors for topsoil CH$_4$ measurements. The goal was to properly capture the CH$_4$ migrations along vertical sections through 0.9 m, 0.6 m, 0.3 m, 0.1 m, and 0m BGS and different lateral locations as shown in Figure (10). Accordingly, the NG detectors were placed in an upright position exactly on top of

the 0.1 m BGS oxygen sensors, letting the two openings protected with wires meshes laying along the vertical axis. This way, it is assumed that the CH_4 migrating upwards passing Oxygen sensors will enter the bottom inlet of NG detectors and eventually enter the atmosphere through the top outlet.

Figure 10: Natural Gas detectors placed at the Urban testbed next to the Structure foundation. The sensor was placed on the soil surface to orient faces with wire meshes along vertical axis. Top surface is having a port for computer connection and power supply wire while bottom is a levelled surface.

Data acquisition

All three sensors (CH_4, humidity/temperature, and absolute pressure) communicate with a microcontroller (Arduino Uno Rev3) to record signals from the sensors along with date and time by a real-time clock (RTC) (DS3231, Diymore) to a microSD card at a frequency of 1 Hz. This facilitates the real time record of surface CH_4 concentrations along with the three influencing environmental parameters.

Standard operation procedure

Based on the sensor performance results, better operation of the MOS requires a minimum preheating period of 24 hrs to stabilize the MOS sensor. This can be achieved by connecting the NG detectors to its designated power source that required for the unit operation. During the field usage, the power supply for the NG detectors were taken via an ethernet cables connected to a NETGEAR POE switch. Accordingly, the sensors were placed and powered one day before the methane release.

The sensor-data acquisition time setup has to be set manually using the pre-developed algorithm by connecting to a computer. Recorded data can be extracted by connecting the microSD card to a computer.

Data analysis

Scripts are written in MATLAB process the collected data. The program enables the users to convert the voltage signals from the MOS to ppmv values, temperature readings in °C, Relative humidity as a percentage (%), and absolute pressure in kPa terms. Here, the users are able to obtain the final readings in 1 second time intervals as well as a 100 second averaged format. Extended details on the NG detector configuration, calibration and field performance validation can be found in Cho et al. (2022).

S2.4 Oxygen sensors for topsoil CH_4 measurement

Oxygen sensors (KE 12 and KE25 series, Figaro USA) were selected to be used for topsoil due to the ease of installation when required and also due to their low cost. Though CH_4 was not the targeted gas for the sensor, use of oxygen as a surrogate to measure other gaseous emissions can be seen in several other studies as shown by Bahlmann et al. (2020), Pourbakhtiar et al. (2017), Poulsen et al. (2018), and Poulsen (2018, 2019). Here, we adopted the methods developed by Bahlmann et al. (2020) to our field experiments through several calibration and conversion steps. In addition to using the sensor as a CH_4 monitoring sensor for this particular study, another intension was to introduce how sensors can be adopted to various applications depending on their availability.

Performance and Calibration

KE-12 and KE-25 are two models of Figaro oxygen sensors with 0-100% oxygen detection range. The two sensors differ each other by their response time and the life expectancy at normal air. The KE-12 series has a response time of 5seconds with an approximate life expectancy of 2.5 years and KE-25 series has a response time of 15seconds with a 5-year average life expectancy. Since the required measurement interval for topsoil methane concentrations was 1minute, the two models were decided to deploy without differentiating. The output of the sensors was given as a mV count ranging from 19.0-35.0 mV and 10.0-15.5 mV for KE-12 and KE-25 sensors respectively. The performance of the sensors for oxygen concentration variations under factory conditions are designed to be linear.

Calibration of the sensors were performed at the laboratory before field deployment. Initially the sensors were connected to the data logger (CR1000, Campbell Scientific, Inc.) using long wires similar to the field. The sensors were then buried under soil compacted inside an airtight 2 L

chamber. The chamber was specially designed with two gas inlets, an outlet for gas exchange and an additional hole for sensor intrusion. Three tubes were placed through the inlet/outlet valves for gas exchange. The sensors were buried under the soil (compacted to METEC field density of $0.48g/cm^3$) inside the chamber and all the wires were taken out through the specific air-tight valve. A datalogger was connected to the computer for continuous monitoring of the mV changes using the PC400 Campbell Scientific software. Varying CH_4 concentrations were achieved using mass flow controllers (MC series, Alicat Scientific) attached to the air and CH_4 gas inlets. The $CH4$ concentration (0–10,000 ppm) in the chamber was set by directly injecting a mixture of pure gases (i.e., zero grade air and ultra-high purity 99.99% CH_4) blended by the controllers. Seven different compositions (100%, 83.33%, 55.6%, 33.4%, 20.0%, 4.78%, and 0% CH_4) were used for the calibration. mV variation of increasing and decreasing concentrations were measured. The mV value shown constantly for 15 mins after changing a composition was chosen as the respective reading for the composition. Shown in Table (3 - 4) and Figure (11) below are calibration results of oxygen sensors.

Table 3: Calibration results for Oxygen sensor - Group1

Time Stamp	CH_4 composition (%)	Sensor mV counts					
		1	2	3	4	5	6
	100	0.34	0.34	0.34	0.34	0.34	0.34
10:08:55 AM	83.33	2.38	2.38	2.38	2.38	2.38	2.38
11:38:41 AM	55.56	5.45	5.45	5.45	5.96	5.79	5.62
7:53:22 PM	33.33	8.51	8.17	8.85	8.85	8.85	8.85
8:51:31 PM	20.00	9.53	9.02	9.87	10.21	9.87	10.21
10:48:53 PM	4.76	10.89	10.55	11.23	11.57	11.4	11.57
	0	11.57	11.23	11.91	12.25	12.25	12.25

Table 4: Calibration results for Oxygen sensor - Group2

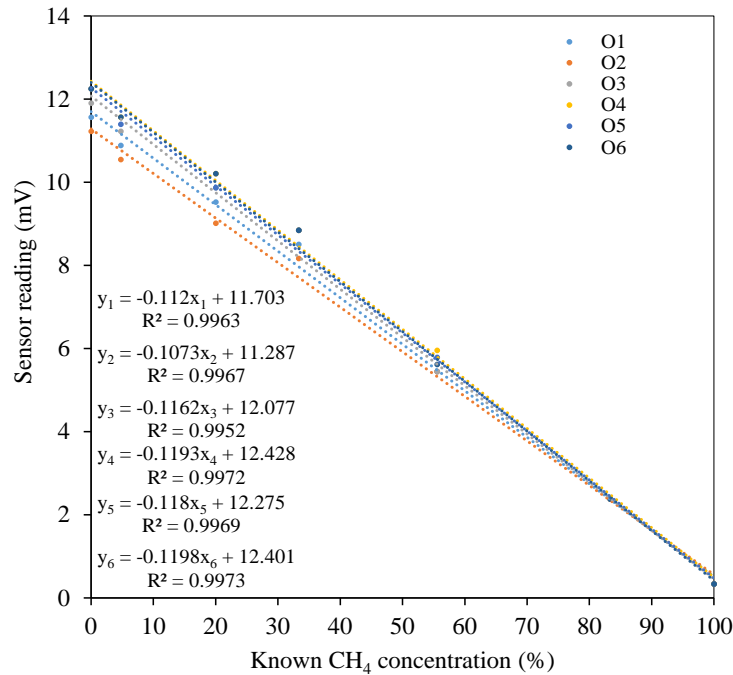| Time Stamp	CH_4 composition (%)	Sensor							
		7	8	9	10	11	12	13	14
	100	0.34	0.34	0.34	0.34	0.34	0.34	0.34	0.34
5:28:14 AM	83.33	1.702	2.04	3.74	1.7	1.87	3.06	3.74	3.74
5:31:07 AM	55.56		3.06	5.11	2.72	3.06	4.76	5.45	5.11
6:06:42 AM	33.33	4.425	4.08	7.49	3.74	4.42	7.15	7.49	7.49
6:43:18 AM	20.00	7.147	7.15	12.25	5.45	7.15	12.25	12.25	12.25
7:10:42 AM	4.76		8.34	14.98	6.13	8.51	14.29	14.98	14.98
	0	8.17	9.19	17.02	6.81	9.19	15.66	17.36	17.02

Figure 11: Calibration curves for Group-1 Oxygen sensors. Best-fit linear equation and the R^2 values for each sensor are also shown.

Best fit curves of the sensor mV counts varied linearly with R^2 values remaining >0.99. Therefore, the calibration equations from each sensor were decided to be used while confirming the possibility of applying two-point calibration when needed.

Field Deployment and Installation

Sensors were buried at 0.1 m BGS depth by turning its sensitive face downwards as shown in Figure (12) below. 0.1 m holes were made next to 0.3 m INIR PVC pipes. Precautions were taken not to disturb the soil unnecessarily. Sensors connected to data wires (to connect to CR1000 datalogger) were buried and residue soil were backfilled and compacted. In addition to that, a control sensor was installed at southwest corner of the testbed to capture the diurnal subsurface oxygen variations during CH_4 releases.

Figure 12: Oxygen sensor installment during a proof-of-concept experiment. The sensor was placed to facing the sensing side downwards. Collocated EC5 soil moisture sensor can also be seen.

Standard operation procedure and Data acquisition

Sensors do not need an additional power supply for operation. 8 sensors were connected to a single datalogger, a program designed for the METEC recordings were set to operate all 8 sensors in parallel with a 1minute data recording interval. Concentration changes were recorded as differential voltage (mV) counts by CR1000 dataloggers. Variation of subsurface oxygen level unaffected by CH_4 was continuously measured for 10days prior to the experiment. Once the CR1000 data logger is powered, the sensors start to record the Oxygen concentrations. However, the use has to make sure some data logger settings are valid for the experiment. Extraction of the recorded data can be done by navigating to the "Download data" window. Here, user will have to create a .txt file with any preferred name beforehand and navigate during the data download process. User can download data as new data sets specific to that particular download or can annex to an existing data file. Care should be taken not to override the data of an existing file.

Data analysis

Conversion of mV values from sensors in to CH_4 concentrations were according to the method introduced by Bahlmann et al. (2020). The applied concept was when the volume of air inside the soil reduces due to the replacement by another gas component, the oxygen sensors react inversely proportional. The relation between the concentrations of additional gas and air introduced by Bahlmann et al. (2020) can be expressed as,

$$C = 100\% - C_{air} = 100\% - \frac{100\%}{21\%} C_{O_2} \tag{9}$$

where C is the concentration of the new gas, C_{air} is the concentration of air, and C_{O2} is the concentration of oxygen. Concentration of oxygen was taken from the conversion of mV counts using the calibration. Here, the 21% of oxygen availability in air has incorporated. However, with the availability of calibration equations, the CH_4 percentage can be found directly without substituting the C_{02} into the equation. The calculations were therefore happened in terms of mV and CH_4 concentrations

It is known that the oxygen concentration of the soils varies diurnally between day and night, meaning that the mV will be varied between day and night. The diurnal variation of mV count was determined during the pre-10 day sensor deployment results. According to this method, there will be a difference in between mV counts of laboratory zero CH_4 and field zero CH_4 measurements. The time specific mV difference was added to the mV readings from the experiments to normalize the zero CH_4 count. By the variation on control sensor mV values, it could be confirmed that diurnal variation of oxygen counts was similar to 10-day pre-deployment period.

S2.5 Environmental Sensor selection

Table 5: Environmental sensor properties

Sensor	TEROS10	TEROS11	TEROS21	Atmos 41	Sonic Young 3D Anemometer	EC5	5TM
Above/ belowground	Below	Below	Below	Above	Above	Below	Below
Range	0.00-0.64 m^3/m^3	0.00 – 0.70 m^3/m^3 -40 - 60°C	-9 to -2,000kPa	Parameter dependent	Parameter dependent	0 - 1.0 m^3/m^3	0 - 1.0 m^3/m^3
Accuracy	±0.03 m^3/m^3	±0.03 m^3/m^3 ±1°C up to 0°C and ±0.5°C upwards	±10	Parameter dependent	Parameter dependent	±0.03 m^3/m^3	±0.03 m^3/m^3
Data logging	External	External	External	External	External	External	External
Size of sensor (cm^2)	38.25		14.4	340	1,190		
Will it work below ground	Yes	Yes	Yes	No	No	Yes	Yes
T operating range (°C)	-40 to 60	-40 to 60	-40 to 60	-50 to 60	-50 to 60	-40 to 60	-40 to 60
RH operating range (%)	0 to 100	0 to 100	0 to 100	0 to 100	0 to 100	0 to 100	0 to 100
Response time	10 ms	25 – 150 ms	150 ms	110 ms	133ms	10ms	150 ms

Table 6: Properties measured by Soil and Atmospheric environmental sensors

Sensor	Data type	Data logger
Teros10	Water content (m^3/m^3)	ZL6
Teros11	Water content (m^3/m^3)	ZL6
	Soil temperature (°C)	
Teros21	Matric potential (kPa)	ZL6
	Soil temperature (°C)	
Atmos41	Wind speed (m/s)	ZL6
	Gust speed (m/s)	
	Air temperature (°C)	
	Vapor pressure (kPa)	
	Atmospheric pressure (kPa)	
	Solar radiation (W/m^2)	
	Precipitation (mm)	
	Maximum precipitation rate (mm/h)	
	Lightning activity	
	Lightning distance (km)	
	Wind direction (°)	
	X-axis level (°)	
	Y-axis level (°)	
	Z-axis level (°)	
MET station	Atmospheric temperature (°C)	OneDrive folder
	Barometric pressure (bar)	
	Relative humidity (%)	
	Sonic temperature (°C)	
	Wind direction (°)	
	Wind elevation (°)	
	Wind speed (m/s)	

S2.6 TEROS10,11, and 12 sensors for soil environmental parameters

TEROS10 (Soil Moisture), TEROS11 (Soil Moisture and Temperature), and TEROS21 (Soil Matric Potential and Temperature) are METER Group, Inc.; USA manufactured environmental sensors used for measuring the belowground environmental parameters.

Performance and Calibration

All TEROS series (Decagon Devices, Inc.; USA) sensors are manufacturer calibrated to fit for most mineral soil types of total porosity (Φ) up to 70 m^3/m^3, while the respective equations can be taken from the manufacturer manuals (User Manual, TEROS10; TEROS12; TEROS21).

Filed Deployment and Installation

Field installation of the sensors were according to a procedure adopted to rural and urban testbeds based on manufacturer installation instructions. All TEROS series (TEROS11, 11, and 21) soil environmental sensors were collocated with INIR sensors at 1.8 m, 0.9 m, and 0.3 m at rural testbed (Figure 2) and 0.9 m, 0.6 m, and 0.3 m depths at urban testbed (Figure 3). During the installation, measures were taken to make sure all measurement points are covered for soil moisture and temperature parameters (soil moisture influence CH_4 migrations while temperature influence CH_4 density). Therefore, TEROS10 and TEROS21 sensors were grouped together while TEROS11 was installed alone.

Installation of sensors happened before passing the 5 cm PVC sleeve for INIR sensors into the holes. The sensors were positioned and pressed into soil by hand with the help of a skinny graduate student. This confirmed that sensors are properly contacted with soil. The data cable of the wires was taken up the soil surface for connecting to ZL6 dataloggers placed aboveground. The sensors were installed permanently, and care was taken during handling to due avoid any soil disturbance or sensor failures. EC5 and 5TM sensors were placed along with oxygen sensors at the urban testbed at 0.1 m depth on a semi-permanent basis. The sensors can be removed when not in used, but with a small frequency in order to avoid frequent topsoil disturbances.

ATMOS41 sensors were installed at 0.05m and 3m above ground at rural testbed while 0.05 m, 0.5 m, and 0.1 m were the installation heights at urban testbed. The sensor was mounted on a tripod and levelled using the water-bubble indicator at the bottom surface of the sensor. The direction of the sensos were set with respect to North using the "N" indication labelled at the sensor surface. The proper fitting to the tripods and the tripod stability were ensured to resist any higher wind conditions.

Standard operation procedure and Data acquisition

Sensors are active when connected to METER Group ZL6 (METER Grup, Inc.; USA) dataloggers. However, some steps were followed to make sure the sensors are working properly, and data recording is according to the required frequency. All sensors were connected to ZL6 data loggers (each datalogger can hold up to 6 sensors). The supporting software provided by the manufacturer (ZENTRA Utility). All ZL6s were set to collect data at every 10minutes. Further details on operation procedures can be found in manufacturer manual (ZL6 User Manual, METER Group)

Data was extracted to a computer and no processing was required as the sensors were set to record in correct units. All soil data were recorded with 10-minute interval while Atmospheric parameters were recorded in 30 second intervals (Atmos41) and MET station with an 8Hz frequency.

Supplementary Material Section 3: Proof-of-concept experiments

S3.1 Environmental Sensor response

Figure (13) below shows the variation of temperature and moisture in the testbed as measured by installed sensors. Both the plots show the variation of temperature and moisture over a period of 24 hrs starting from mid night. They represent variation during different scenarios created at the site. First, it is necessary to understand the variation of temperature through the profile starting from atmosphere towards the gas source. The sensor matrix installed as allowed researchers to capture these variations simultaneously as shown in Figure (13a). From the figure, it is clearly visible how the temperature of top-soil layer is affected by the atmospheric changes in temperature while lower layers are not affected. The availability of temperature variations will help in better understanding whether it is a temperature-controlled gas density change or is it an atmospheric variation influenced topsoil variation.
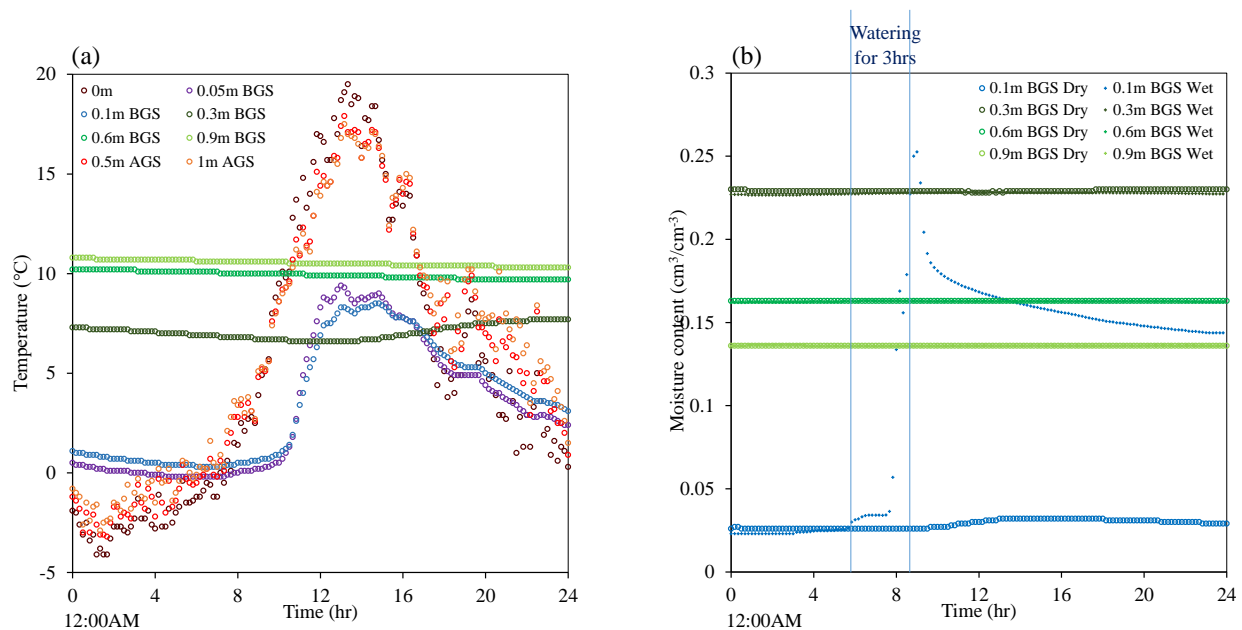

Figure 13: Variation of (a) Temperature across Atmosphere-surface-subsurface and (b) Soil moisture content for a 24 hr span during two proof-of-concept experiments

Figure (13b) shows how the soil moisture content of 0.1m BGS layer has changed during the 3hr watering event. The intention of this specific controlled watering was to increase the moisture of

top-soil layer while lower layers remain at a constant moisture level. Therefore, it is confirmed that the testbed is capable of creating different moisture related variations as well as measuring them properly.

S3.2 Subsurface and Surface Methane Variations

The following figure (14) shows the (a) subsurface (15 cm BGS) and (b) surface (0cm ABS) methane concentration variations measured using oxygen and NG detectors respectively, and (c) Atmospheric temperature and wind speed variations measured using Atmos 41 during the 2 splm release continued for 5 days and 1 day of No-release follow-up measurement. The results show how the methane concentrations are getting reduced with the distance (1 m and 2 m East) from the release in both subsurface and surface as wells as how the concentrations have fluctuated diurnally with atmospheric variations. Similar observations were made by Forde et al. (2019) and the patterns are complying with the explanations by Massmann and Farrier (1992) and Xu et al. (2014).
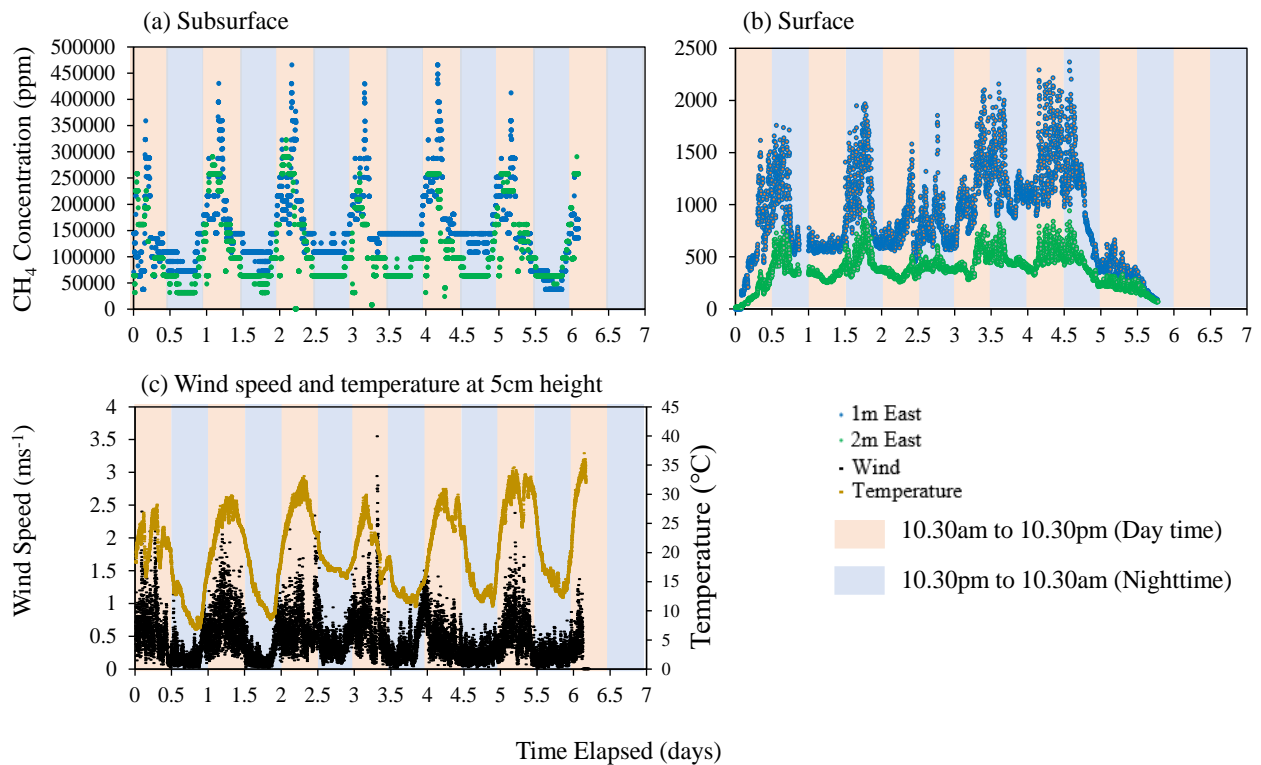

Figure 14: Variation of methane concentration at (a) Subsurface at 5 cm BGS measured using Oxygen sensors, (b) Surface measured using NG detectors, and (c) Wind speed and Atmospheric Temperature variation during a 2 slpm proof of concept release

Further, shown below are the surface plots generated during the same experiment, as measured by entire network of subsurface (Oxygen) and Surface (NG detectors) sensors. These surface plots show how the shape of the plume change when coming migrating upwards towards the surface.
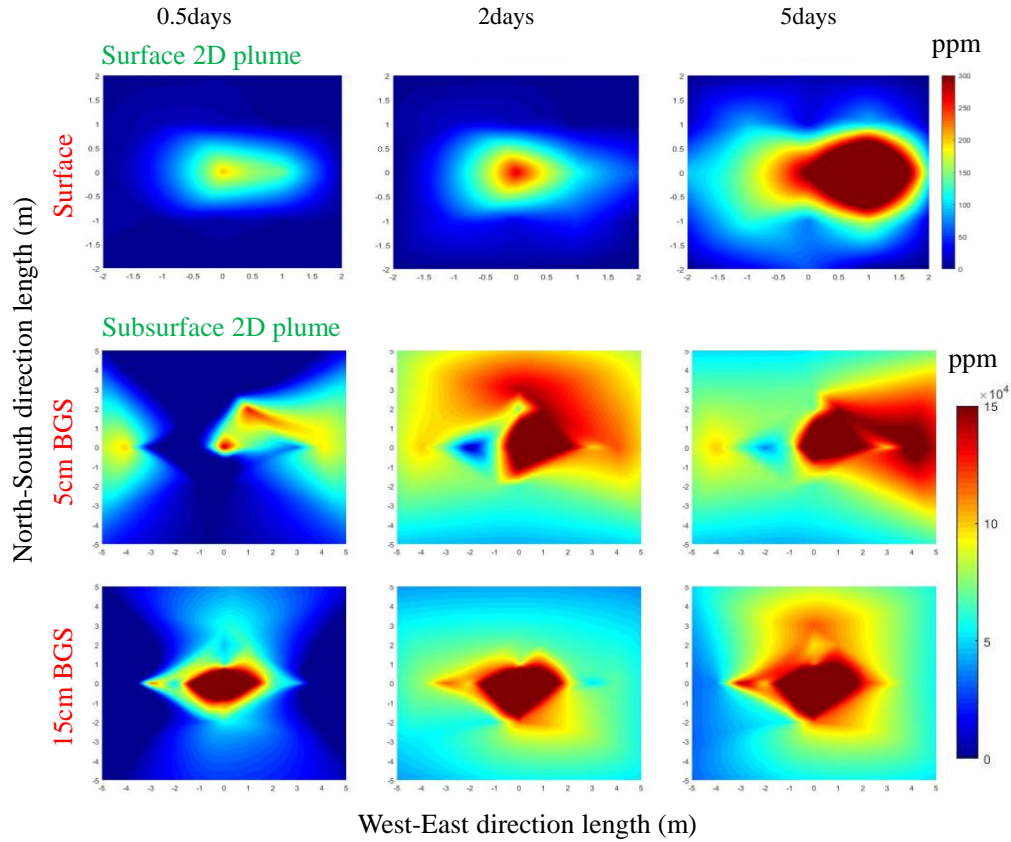

Figure 15: 2D methane plume patterns at Surface and Subsurface at 5 cm & 15 cm BGS measured using NG detectors and Oxygen sensors respectively during the 2 slpm proof-of-concept experiment

Further, these plume patterns demonstrate the variety of environmental conditions to be tested over the course of this experiment. Importantly, the testbed's capability of continuous measurements of methane and other variables over time and space has also been proven at this stage.

References

3D Ultrasonic Anemometer 81000RE / 81000VRE Information, R.M. Young Company. Available at https://www.youngusa.com/product/ultrasonic-anemometer-3/ Accessed on 10 January 2022

5TM User Manual, METER Group Inc. Available at METER Group website http://publications.metergroup.com/Manuals/20424_5TM_Manual_Web.pdf. Accessed on 10 January 2022

Atmos41 User Manual. METER Group Inc. Available from http://library.metergroup.com/Manuals/20635_ATMOS41_Manual_Web.pdf Accessed on 10 January 2022

Bell, C S, T. Vaughan, and D. Zimmerle. 2020. Evaluation of next generation emission measurement technologies under repeatable test protocols. Elem Sci Anth, 8: 32. DOI: https://doi.org/10.1525/elementa.426

Bahlmann, l.m., K.M. Smits, K. Heck, E. Coltman, R. Helmig, and I. Neuweiler. 2020. Gas component transport across the different soil-atmosphere interface for gases of different density: Experiments and modeling. Water Resources Research 56(9): e2020WR027600. http://dx.doi.org/10.1029/2020WR027600

Chamindu Deepagoda, T. K. K., Smits, K. M., & Oldenburg, C. M. (2016). Effect of subsurface soil moisture variability and atmospheric conditions on methane gas migration in shallow subsurface. *International Journal of Greenhouse Gas Control*, *55*, 105–117. https://doi.org/10.1016/j.ijggc.2016.10.016

Cho, Y., K.M. Smits, S.N. Riddick, and D.J. Zimmerle. 2022. Calibration and filed deployment of low-cost sensor network to monitor underground pipeline leakage. Sensors and Actuators B: Chemical. Doi: 10.1016/j.snb.2021.131276

Cho, Y., B.A. Ulrich, D.J. Zimmerle, K.M. Smits, Estimating natural gas emissions from underground pipelines using surface concentration measurements, Environ. Pollut. 267 (2020), 115514, https://doi.org/10.1016/j.envpol.2020.115514

EC5 User Manual. METER Group Inc. Available from http://publications.metergroup.com/Manuals/20431_EC-5_Manual_Web.pdf Accessed on 10 January 2022

Electronic Code of Federal Regulations §192.327 Cover. 2021. E-CFR. Available at Western Regional Gas Conference website: https://www.ecfr.gov/cgibin/retrieveECFR?gp¼1&SID¼c3b0e911814b61c0f807c43f51ac7bc6& ty¼HTML&h¼L&mc¼true& r¼SECTION&n¼se49.3.192_1327. Accessed 6 January 2021

Forde, O. N., A.G. Cahill, R. D. Beckie, and K. U. mayer. 2019. Barometric-pumping controls fugitive gas emissions from a vadose zone natural gas release. *Scientific reports* 9.1 (2019): 1-9.Doi: 10.1038/s41598-019-50426-3 1

Gao, B., M. K. Mitton, C. Bell, D. Zimmerle, T. K. K. Chamindu Deepagoda, A. Hecobian, and K. M. Smits. 2021. Study of Methane Migration in the Shallow Subsurface from a Gas Pipe Leak. Elem Sci Anth, 9: 1. DOI: https://doi.org/10.1525/ elementa.2021.00008

Jayarathne, J.R.R.N., Deepagoda, T.K.K.C., Clough, T.J., Nasvi, M.C.M., Thomas, S., Elberling, B., Smits, K.: Gas-Diffusivity based characterization of aggregated agricultural soils. Soil Sci. Soc. Am. J. 84(2), 387–398 (2020). doi. org/ 10. 1002/ saj2.20033

Maxell Oxygen Sensors KE-Series, Product Information, Figaro USA. Inc. Available from https://www.figarosensor.com/product/docs/ke_product%20infomation%28fusa%29_rev06.pdf Accessed on 10 January 2022

Poulsen, T. G., Furman, A.,&Liberzon, D. 2018. Effect of near-surface wind speed and gustiness on horizontal and vertical porous medium gas transport and gas exchange with the atmosphere. *European Journal of Soil Science*, *69*(2), 279–289. https://doi.org/10.1111/ejss.12531

Poulsen, T. G. (2018). Measuring horizontal pore gas velocity profiles in porous media in response to near-surface wind speed and gustiness.

Poulsen, T. G. (2019). Linking below-surface horizontal pore velocity profiles in porous media with near-surface wind conditions and

Pourbakhtiar, A., Poulsen, T. G., Wilkinson, S., & Bridge, J. W. 2017. Effect of wind turbulence on gas transport in porous media: Experimental method and preliminary results. *European Journal of Soil Science*, *68*(1), 48–56. https://doi.org/10.1111/ejss.12403

TEROS 10 User manual. METER Group Inc., USA. Available from http://publications.metergroup.com/Manuals/20788_TEROS10_Manual_Web.pdf Accessed on 10 January 2022

TEROS 11/12 INTEGRATOR GUIDE, METER Group Inc., USA. Available from http://publications.metergroup.com/Integrator%20Guide/18224%20TEROS%2011-12%20Integrator%20Guide.pdf Accessed on 10 January 2022

TEROS 21 GEN 1 INTEGRATOR GUIDE. METER Group Inc., USA. Available from http://library.metergroup.com/Integrator%20Guide/18204%20TEROS%2021%20Gen1%20Integrator%20Guide.pdf Accessed on 10 January 2022

Ulrich, B.A., Mitton, M., Lachenmeyer, E., Hecobian, A., Zimmerle, D., Smits, K.M., 2019. Natural Gas Emissions from Underground Pipelines and Implications for Leak Detection. Environ. Sci. Technol. Lett. 6, 401–406. https://doi.org/10.1021/acs.estlett.9b00291

Zimmerle, D., T. Vaughn, C. Bell, K. Bennet, P. Deshmukh, E. Thoma. 2020. Detection Limits of Optical Gas Imaging for Natural Gas Leak Detection in Realistic Controlled Conditions. *Environmental Science and Technology*.55,8583-8591. Doi:10.1021/acs.est.1c00859

ZL6 User Manual. METER Group Inc., USA. Available from http://publications.metergroup.com/Manuals/20789_ZL6_Manual_Web.pdf Accessed on 10 January 2022

Xu, L., Lin, X., Amen, J., Welding, K. & McDermitt, D. 2014 Impact of changes in barometric pressure on landfill methane emission. *Glob.Biogeochem. Cycles* 28, 2013GB004571

Massmann, J. & Farrier, D. F. 1992. Effects of atmospheric pressures on gas transport in the vadose zone. *Water Resour. Res.* 28, 777–791